

Effect of β -O-Glycosylation on L-Ser and L-Thr Diamides: A Bias toward α -Helical Conformations

Francisco Corzana,^[a] Jesús H. Busto,^[a] Søren B. Engelsen,^[b] Jesús Jiménez-Barbero,^[c] Juan L. Asensio,^[d] Jesús M. Peregrina,^[a] and A. Avenoza*^[a]

Abstract: β -D-O-glycosylation produces a remarkable effect on the peptide backbone of the model peptides derived from serine and threonine. Consequently, this type of glycosylation is responsible for the experimentally observed shift from extended conformations (model peptides) towards the

folded conformations (model glycopeptides). The conclusion has been solidly assessed by a combined NMR/MD pro-

ocol. Interestingly, the MD (molecular dynamics) results for the glycopeptides point towards the existence of water-bridging molecules between the sugar and peptide moieties, which could explain the stabilization of the folded conformers in aqueous solution.

Keywords: conformation analysis • glycopeptides • molecular dynamics • NMR spectroscopy • peptides

Introduction

The physical and biological properties that O-glycosylation confers to the protein to which the sugars are attached are well described in several reviews on the biosynthesis, structures and functions of O-glycosylation.^[1] Logically, these properties include conformational alterations of the protein structures. The most common O-glycosylations involve the α -O-glycosidic linkage of GalNAc attached to a Ser/Thr-rich domain (mucin-type)^[2] or the β -O-glycosidic linkage of GlcNAc linked to a Ser/Thr residue of cytoplasmic and nuclear proteins, which play a regulatory role in protein function.^[3] In contrast, some specific types of O-glycosylation,

such as the β -O-linked attachment of D-Glc to Ser/Thr (O-glycosylation) are less frequent and have been found in the epidermal growth factor (EGF) domains of different serum proteins^[4a-d] and the Notch receptor.^[4e-g] The role of the glucose in these systems is unknown and remains controversial. In addition, in the field of unnatural glycopeptides as therapeutics, a glycosylated form of enkephalin Tyr-Thr-Gly-Phe-Leu-Ser peptide, in which a β -D-Glc has been appended to the Ser residue, produces analgesic effects similar to morphine.^[5] On the one hand, it is well appreciated that in nature, the α -O-glycosylation with GalNAc and higher oligosaccharides have a profound organizational effect on the underlying peptide backbone, forcing it into an extended conformation.^[6] On the other hand, other authors have suggested that glycosylation per se has no effect on the peptide backbone conformation, in the absence of amide groups at the sugar moiety.^[7]

Thus, taking into account these features, it seems essential to improve our perception of the mechanisms that allow the carbohydrate to modify the conformational equilibrium of the peptide backbone to properly understand the key biological processes in which glycopeptides are involved, such as enzymatic catalysis, hormonal control, transport, cell adhesion or cell-cell recognition.^[8]

On this basis, as a first step to evaluate the implications that β -O-glycosylation has on the peptide conformation, we decided to conduct the synthesis and the structural (NMR and modelling) analysis of the L-Ser diamide (Ac-L-Ser-NHMe, **1**) and L-Thr diamide (Ac-L-Thr-NHMe, **2**) as reference model peptides, as well as the simplest glycopeptide

[a] Dr. F. Corzana, Dr. J. H. Busto, Dr. J. M. Peregrina, Dr. A. Avenoza
Departamento de Química, Universidad de La Rioja
UA-CSIC. 26006 Logroño (Spain)
Fax: (+34) 941-299-655
E-mail: alberto.avenoza@dq.unirioja.es

[b] Dr. S. B. Engelsen
The Royal Veterinary and Agricultural University
Rolighedsvej 30, 1958 Frederiksberg C (Denmark)

[c] Prof. J. Jiménez-Barbero
Centro de Investigaciones Biológicas (C.S.I.C.)
Ramiro Maeztu 9, 28040 Madrid (Spain)

[d] Dr. J. L. Asensio
Instituto de Química Orgánica (C.S.I.C.)
Juan de la Cierva 3, 28006 Madrid (Spain)

Supporting information for this article is available on the WWW under <http://www.chemeurj.org/> or from the author.

derivatives Ac-L-Ser(β -D-Glc)-NHMe (**1g**) and Ac-L-Thr(β -D-Glc)-NHMe (**2g**, Figure 1). In this context, it is important to note that computational studies on these systems are not trivial. Indeed, the currently used all-atom force fields that

only two cases, the structural studies were carried out in water solution.^[11c,d]

Results and Discussion

Synthesis: Derivatives **1** and **2** were easily obtained from the corresponding natural amino acids as described in the Supporting Information.

Glycopeptides **1g** and **2g** were obtained by using the standard conditions of the Koenigs–Knorr glycosylation. Therefore, compounds **1** and **2** were treated with 2,3,4,6-tetra-*O*-benzoyl- α -D-glucopyranosyl bromide in presence of silver triflate and dichloromethane. Under these conditions, the reaction gave exclusively the corresponding β -anomers in a moderate yield. Finally, the hydrolysis of the benzoyl groups with sodium methoxide in methanol gave the desired compounds **1g** and **2g** (Scheme 1).

Geometry of the backbone: Our conformational study of compounds **1**, **2**, **1g** and **2g** has involved the use of NOE-based distance information and homonuclear coupling constants, which have been interpreted with the assistance of MD-tar (molecular dynamics with time-averaged restrains) simulations.^[12] Under these conditions, the conformational

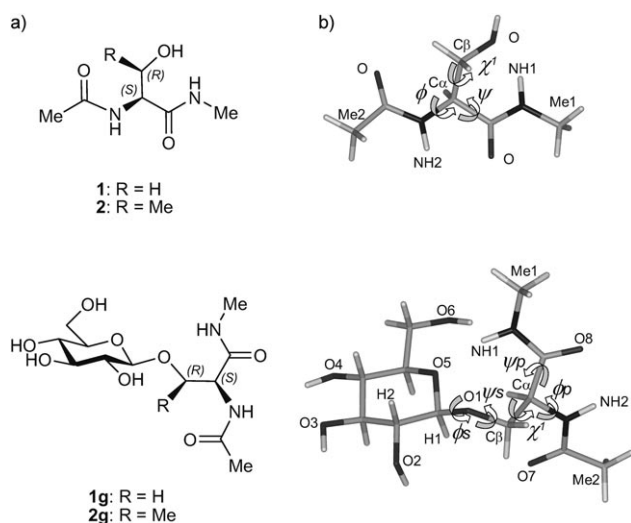
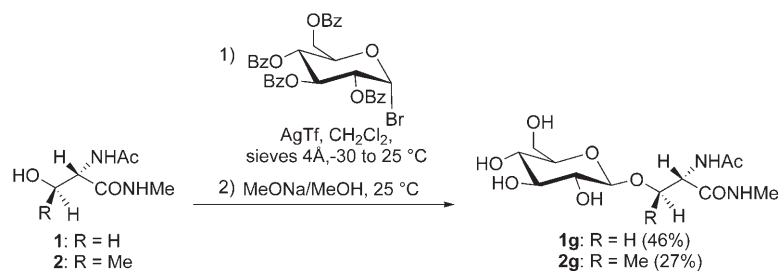


Figure 1. a) Structure of model peptides **1** and **2** and glycopeptides **1g** and **2g**. b) 3D structure of **1** and **1g**, including the atomic and dihedral labels employed in this work.

predict reasonable conformational dynamics for larger peptides or proteins fail to reproduce the measured conformational distribution for di- and tripeptide systems and vice versa.^[9] As a consequence, the conformational study of small model glycopeptides reported to date is rather limited. Moreover, these studies^[6,7,10,11] include mainly small glycopeptides, with α -D-GalNAc or β -D-GlcNAc. Investigation of glycopeptides containing Glc is limited to a few studies and, in



Scheme 1. Synthetic routes to **1g** and **2g**.

regions sampled by the simulations (within the sterically allowable regions) are mainly determined by the experimental constraints and the fine details of the simulation are not critical.

As a first step in the structural study of the model peptides **1** and **2** and glycopeptides **1g** and **2g**, selective 1D NOESY experiments in D₂O (see Supporting Information) and 2D NOESY experiments (Figure 2) in H₂O/D₂O 9:1 were carried out for all the compounds. In addition, ³*J*(H α ,H β) and ³*J*(NH₂,H α) coupling constants were measured for the peptides and glycopeptides.

The exhaustive study of the 2D NOESY spectra corresponding to the model peptides **1** and **2** in H₂O/D₂O 9:1 reveals that they present similar patterns of NOEs. Moreover, the strong *d*(H α ,NH1) NOE observed, along with the absence of the *d*(NH1,NH2) one, suggests the existence of extended conformations in the peptide backbone^[13] (Figure 2a). However, in model glycopeptides **1g** and **2g**, the

Abstract in Spanish: La β -D-O-glucosilación de péptidos modelo derivados de serina y treonina afecta notablemente a la estructura de dichos péptidos. De hecho, esta glicosilación es responsable del cambio, experimentalmente observado, de conformaciones extendidas (péptidos modelo) a conformaciones plegadas (glicopéptidos modelo). A esta conclusión se ha llegado combinando experimentos de RMN con cálculos de dinámica molecular. Es importante destacar que los resultados obtenidos mediante estos cálculos apuntan hacia la existencia de moléculas de agua que enlazan las partes peptídica y carbohidrato del glicopéptido. Dichas moléculas de agua podrían explicar la estabilización de las conformaciones plegadas observadas en disolución acuosa.

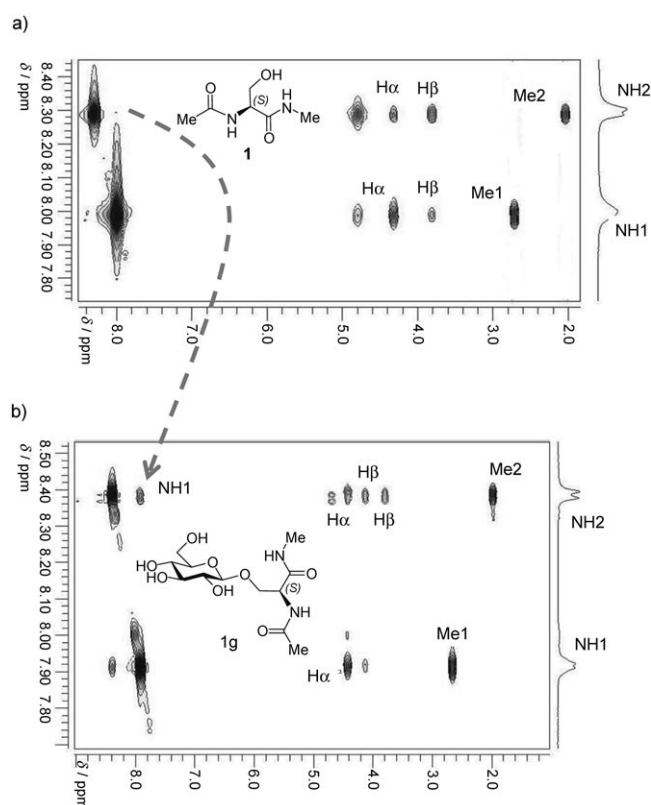


Figure 2. Section of the 800 ms 2D NOESY spectra (400 MHz) in H₂O/D₂O 9:1 at 25 °C of model peptide **1** (a), and model glycopeptide **1g** (b), showing the amide cross-peaks.

medium $d(\text{H}\alpha, \text{NH}1)$ NOE observed, together with the medium $d(\text{NH}1, \text{NH}2)$ NOE, suggest the coexistence of extended and folded conformers (Figure 2b).

To get an experimentally derived ensemble, 80 ns MD-tar simulations were carried out by inclusion of the experimental distances and $^3J(\text{NH}2, \text{H}\alpha)$ and $^3J(\text{H}\alpha, \text{H}\beta)$, as time-averaged restraints. The experimentally determined distances were derived from the corresponding NOE build-up curves^[14] (see Supporting Information). Additionally, distances involving NH protons were semiquantitatively determined by integrating the volume of the corresponding cross-peaks. The 3J coupling constants derived from the simulations were estimated by using the appropriate Karplus equation.^[15]

The MD-tar were performed by using AMBER version 6.0.^[16] The ff94^[17] force field was implemented with the new GLYCAM 04 parameters,^[18] to accurately simulate the conformational behaviour around the sugar moiety. For comparison, the ff99^[19] and a modified ver-

sion of ff99 (ff99')^[20] force fields were also tested with compounds **1** and **1g**, obtaining similar results with the three force fields (see Supporting Information). In addition, 10 ns unrestrained MD simulations in explicit water (MD-free) were performed for compounds **1** and **1g** (see Tables 1 and 2 and Supporting Information).

Table 1. Comparison of the experimental (NMR) and simulated (MD) distances and 3J couplings for **1** and **2**.^[a]

	Exptl ^[b]	peptide 1		peptide 2	
		MD-free ff94	MD-tar	Exptl ^[b]	MD-tar
$d(\text{NH}1, \text{NH}2)$	absent (>3.0)	2.4	3.0	absent (>3.0)	3.2
$d(\text{H}\alpha, \text{NH}1)$	s (2.3)	3.1	2.4	s (2.3)	2.4
$d(\text{H}\alpha, \text{NH}2)$	m (2.7)	2.9	2.9	m (2.5)	2.9
$^3J(\text{H}\alpha, \text{H}\beta)$ ^[c]	5.7	10.7/3.4	5.4	4.2	4.1
$^3J(\text{NH}2, \text{H}\alpha)$ ^[d]	6.3	6.5	6.5	7.3	7.0

[a] Distances are given in Å and 3J coupling in Hz. [b] w=weak, m=medium and s=strong NOE. [c] Experimentally observed as a pseudotriplet and estimated by using the Karplus equation given in reference [15a] [d] Estimated by using the Karplus equation given in reference [15b].

Table 1 gathers all the relevant NOE-derived distances and 3J values, together with those obtained from unrestrained (MD-free) and MD-tar simulations for the model peptides **1** and **2**.

As shown in Table 1, the unrestrained MD simulations suggest folded conformations ($d(\text{NH}1, \text{NH}2) < d(\text{H}\alpha, \text{NH}1)$) for the backbone.^[9] However, and according to the NMR data (distances and $^3J(\text{H}\alpha, \text{H}\beta)$ values), they fail to satisfactorily reproduce the conformation of the peptide backbone of **1**. On the other hand, the distances and 3J calculated values from the MD-tar simulations are in very good agreement with the experimental ones.

Figure 3a shows the Φ/Ψ distributions for the peptide backbone in **1** and **2** obtained from the MD-tar simulations. It can be observed that according to the NOE experiments

Table 2. Comparison of the experimental and MD simulations derived distances and 3J couplings for glycopeptides **1g** and **2g**.^[a]

	Exptl ^[b]	glycopeptide 1g		glycopeptide 2g	
		MD-free ff94	MD-tar	Exptl ^[b]	MD-tar
$d(\text{NH}1, \text{NH}2)$	m (2.7)	2.2	2.5	s (2.3)	2.2
$d(\text{H}\alpha, \text{NH}1)$	s (2.3)	3.2	2.5	m (2.5)	2.5
$d(\text{H}\alpha, \text{NH}2)$	m (2.6)	2.9	2.9	m (2.8)	2.9
$d(\text{H}\beta_{\text{pro-S}}, \text{NH}2)$	m (2.9)	2.8	2.7	m (2.9)	2.9
$d(\text{H}\beta_{\text{pro-R}}, \text{NH}2)$	m (2.8)	2.9	2.8	m ^[c]	3.0
$d(\text{H}\beta_{\text{pro-S}}, \text{H}\alpha)$	2.6	2.6	2.5	m	2.5
$d(\text{H}\beta_{\text{pro-R}}, \text{H}\alpha)$	2.6	2.5	2.5	m ^[c]	2.9
$d(\text{H}\beta_{\text{pro-S}}, \text{H}1)$	2.6	2.6	2.6	2.6	2.3
$d(\text{H}\beta_{\text{pro-R}}, \text{H}1)$	2.3	2.4	2.4	2.4 ± 0.5 ^[c]	3.2
$^3J(\text{H}\alpha, \text{H}\beta)$ ^[c]	4.6	6.4/4.4	5.1	3.4	3.5
$^3J(\text{NH}2, \text{H}\alpha)$ ^[d]	6.9	6.9	6.8	7.5	7.5

[a] Distances are given in Å and 3J coupling in Hz. [b] The w=weak, m=medium and s=strong NOE. [c] Experimentally observed as a pseudotriplet and estimated by using the Karplus equation given in reference [15a]. [d] Estimated by using the Karplus equation given in reference [15b]. [e] In compound **2g**, H($\beta_{\text{pro-R}}$) must be substituted by β -Me of Thr.

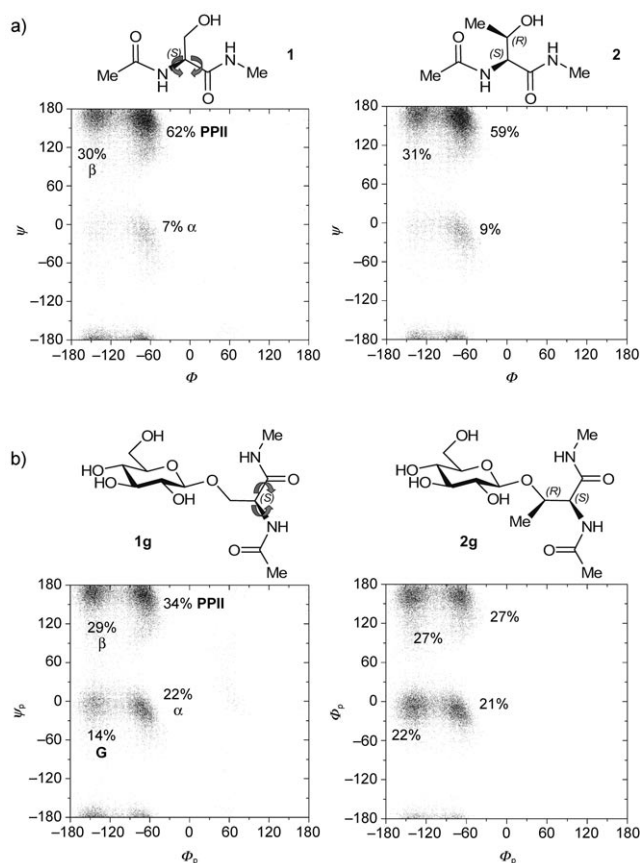


Figure 3. Φ/Ψ distributions obtained from the MD-tar simulations for the peptide backbone of peptides **1** and **2** (a), and glycopeptides **1g** and **2g** (b).

mentioned above, the Φ/Ψ dihedral values (backbone) of model peptides **1** and **2** are similar to those typical for extended conformations, such as PPII ($\sim 60\%$) and β -sheet ($\sim 30\%$), and only a small amount of conformers showed Φ/Ψ dihedral values corresponding to a α -helical structure ($< 10\%$). This result is in agreement with the structure found in aqueous solution for other small peptides.^[21]

The next step was to investigate the conformational preferences of the target model glycopeptides **1g** and **2g** in water. Thus, Table 2 gathers the relevant NOE-derived distances and 3J values, together with those obtained from unrestrained (MD-free) and MD-tar simulations for these model glycopeptides.

As can be seen in Table 2, although the MD-free simulations on **1g** reproduce most of the experimental data, a non-realistic high percentage of folded conformers (α -helix and G conformers)^[22] is predicted (as deduced from the computed large $d(\text{H}\alpha, \text{NH}1)$ and small $d(\text{NH}1, \text{NH}2)$ distances).

Figure 3b shows the Φ_p/Ψ_p distributions obtained for the backbone of glycopeptides **1g** and **2g** from the MD-tar simulations. Interestingly, the β -O-glucosylation strongly perturbs the peptide backbone of the model glycopeptides derived from natural amino acids. Consequently, for glycopeptides **1g** and **2g**, there is an important shift from extended

conformations towards folded conformations (α -helix and G). This finding is, as commented above, experimentally corroborated by the medium-size NOE for $d(\text{NH}1, \text{NH}2)$.

Geometry of the side chain: Concerning the side chain χ^1 torsional angle, the model peptide **1** mainly adopts the three lowest energy staggered rotamers, denoted as *gauche*($-$) or *g*($-$) ($\chi^1 \sim -60^\circ$), *gauche*($+$) or *g*($+$) ($\chi^1 \sim 60^\circ$) and *anti* or *t* ($\chi^1 \sim -180^\circ$), with a similar population in aqueous solution (Figure 4a).

The methyl group at the β -position of the threonine derivative constrains the lateral chain and, consequently, in model peptide **2**, χ^1 torsional angle exhibits mainly the *g*($+$) conformation with a significant decrement of the *g*($-$) rotamer. This result is in good agreement with the experimentally observed $J(\text{H}\alpha, \text{H}\beta)$. Thus, the larger J found in **1** (5.7 Hz in comparison to 4.2 Hz) suggests more flexibility for the side chain.^[15a] Moreover, the major *g*($+$) conformer found in **2** is in accordance with the NOE observed between $\text{Me}\beta$ and $\text{NH}2$ (see Supporting Information). This behaviour of the side chain is somehow similar to that found by Hruby et al.^[23] for serine and threonine in regular proteins.

Another consequence of the β -O-glucosylation is related to the lateral chain of the amino acid moiety (Figure 4b). Thus, while in glycopeptide **1g** the χ^1 dihedral shows a similar distribution to that of its parent peptide **1**, glycopeptide **2g** differs significantly from **2**. Consequently, in **2g**, χ^1 mainly adopts the *g*($+$) (44%) and the *t* (47%) conformations, while in derivative **2** the *g*($+$) conformer is mainly populated (72%).

Geometry of the glycosidic linkage: With regard to the sugar moiety, Figure 5 shows the Φ_s/Ψ_s distribution for the glycosidic linkage of the model glycopeptides **1g** and **2g** obtained from the MD-tar simulations. The most significant feature is that the glycosidic linkage is rather rigid in both compounds. As can be seen, Φ_s exhibits a value close to -60° in both molecules, which is in accordance with the exoanomeric effect,^[24] while Ψ_s takes mainly a value close to 180° in **1g**, while in **2g**, and due to the $\text{Me}\beta$, the value is slightly different (around 140°).

Anisotropic hydration of glycopeptide 1g: Finally, to shed some light on the factors that govern the experimentally observed shift to the folded conformations in the model glycopeptides, we carried out an extensive theoretical study on glycopeptide **1g**. Therefore, and assuming that the unrestrained MD simulation (MD-free ff94, Table 2) is somehow representative of folded conformations in aqueous solutions, the first step was to investigate the hydrogen bonds between the sugar and the peptide moieties. As result, no significant hydrogen bonds were detected between the peptide and sugar moieties over the course of the MD-free simulation, which is in accordance with the MD-tar simulations. In fact, the most persistent one was present only 4% of the trajectory time and involves oxygens O6 and O8 ($\text{O}\cdots\text{O}$ distance $> \text{or} = 3.3 \text{ \AA}$).

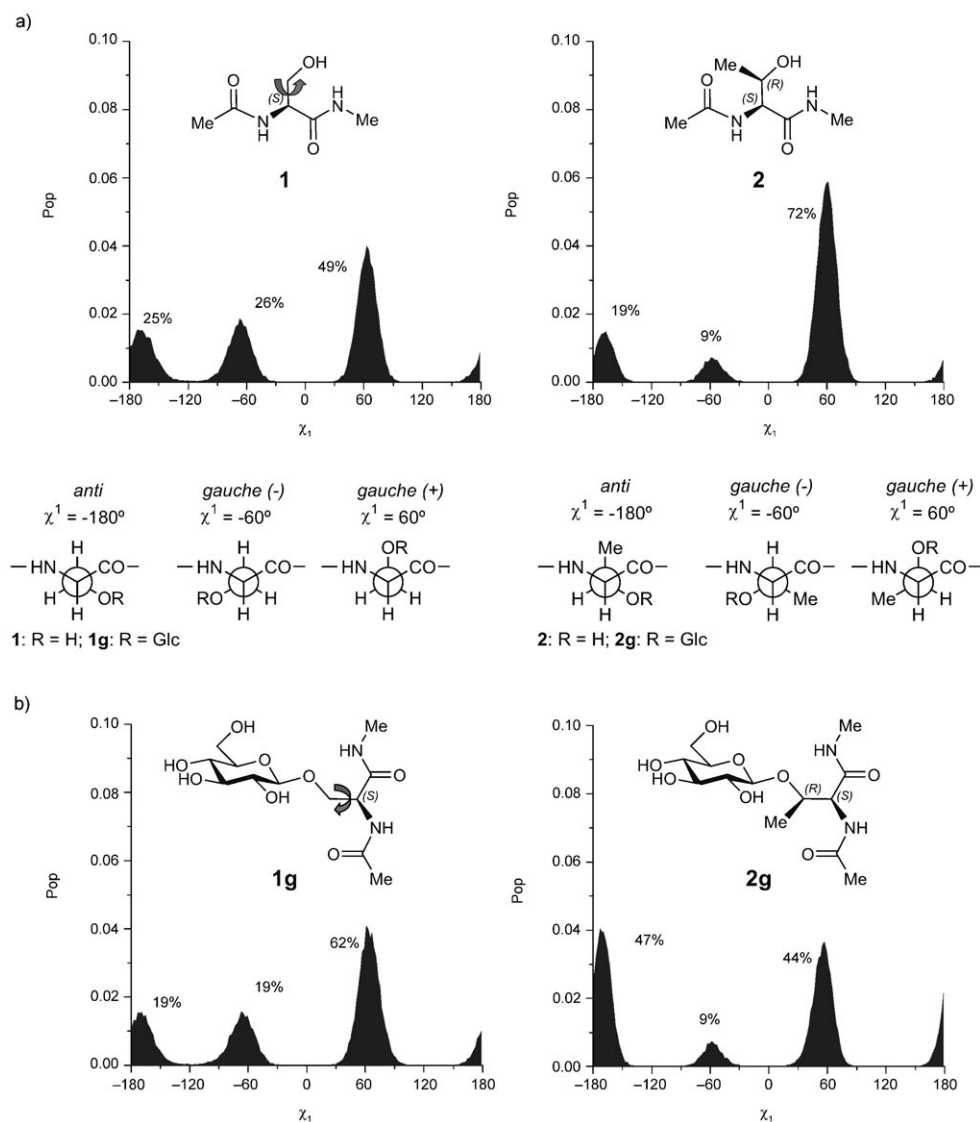


Figure 4. χ^1 distributions obtained from the MD-tar simulations for model peptides **1** and **2** (a), and model glycopeptides **1g** and **2g** (b).

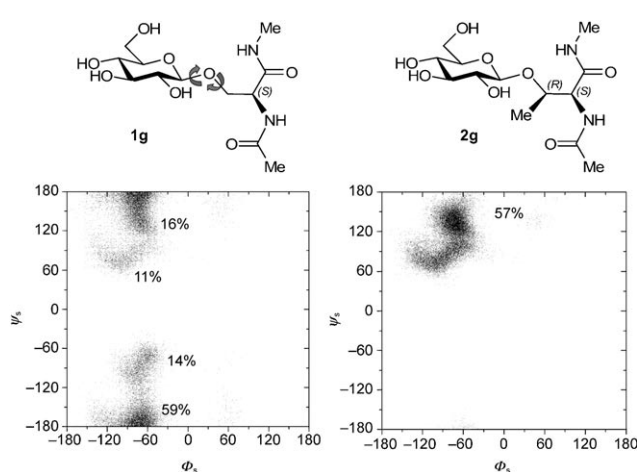


Figure 5. Φ_s/Ψ_s distributions obtained from the MD-tar simulations for the glycosidic linkage of glycopeptides **1g** and **2g** ($\Phi = \text{O5-C1-O1-C}\beta$, $\Psi = \text{C1-O1-C}\beta\text{-C}\alpha$).

To gain detailed knowledge about the influence of water upon the folded conformations, we initially calculated the number of water molecules in the first hydration shell. This number was 18.3 or 5.0, depending on the distance considered between the solute and water molecules, 3.5 or 2.8 Å, respectively. These values are similar, for example, to that found in disaccharide methyl- α -D-maltoside.^[25a] The next stage was to inspect the anisotropic hydration of the solute in these free trajectories. In this sense, and taking into account that the GLYCAM 04 force field exhibits reasonably structured solute-water interactions,^[25] (see Supporting Information), the normalised two-dimensional radial pair distributions^[26] were calculated for all possible shared water density sites ($\text{Os1}\cdots\text{Ow}\cdots\text{Os2}$ and $\text{Os}\cdots\text{Ow}\cdots\text{N}$), in which Ow is the water oxygen and Os and N are solute oxygen or nitrogen, respectively.

The most populated intraresidue water bridge found for **1g** was accommodated between atoms $\text{O2}\cdots\text{N2}$, which is

present about 24% of the time. The maximum density of this shared water site was 4.2 times the bulk density (Figure 6), producing maximum and average residence times

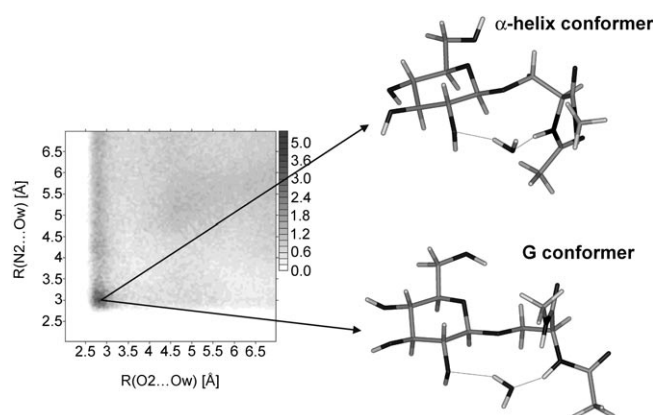


Figure 6. Two-dimensional radial pair distribution functions of different water-bridging situations found in the unrestrained 10 ns MD simulations for glycopeptide **1g**.

of 10.0 and 1.3 ps, respectively. The average distance O2...N2 was 4.9 Å, ranging from 6.9 to 2.7 Å. As can be seen in Figure 6, the water-bridging molecules are present in both folded conformers. Furthermore, when this water bridge is present, χ^1 dihedral exhibits a value close to 60°, which is the most populated in both the MD-free and MD-tar of **1g**. Additionally, other less significant water bridges (present about 10% of the time) were found between O5...N2, which is mainly found in the α -helix conformer, and another one in the G conformation between atoms O6...O8. While in the carbohydrates field the existence of these water-bridging molecules have been considered responsible for their conformational preferences,^[25a,h] to the best of our knowledge, this is the first time that these structural water molecules have been found in glycoamino acid derivatives.

We also studied the conformational behaviour of these relatively small systems by quantum mechanical approaches. Therefore, to obtain the optimised geometry of **1g**, its conformational space was deeply explored by means of semiempirical methods (AM1).^[27] As a result, the lowest energy structure found was fully optimised at the B3LYP/6-31G(d) level^[28] in vacuo. The backbone of this global minimum structure corresponds to a γ_L -turn motif, which is in accordance with the most stable ab initio conformer of α -D-GalNAc-Ac-L-Ser-NHMe previously calculated by Csonka et al (Figure 7a).^[29] Nevertheless, this conformation is not experimentally observed in aqueous solution as deduced from our NMR/MD protocol. Therefore, it is important to note that great care must be taken when the conformational behaviour of these flexible molecules are studied by using quantum mechanical methods in which the solvent is not taken into account.

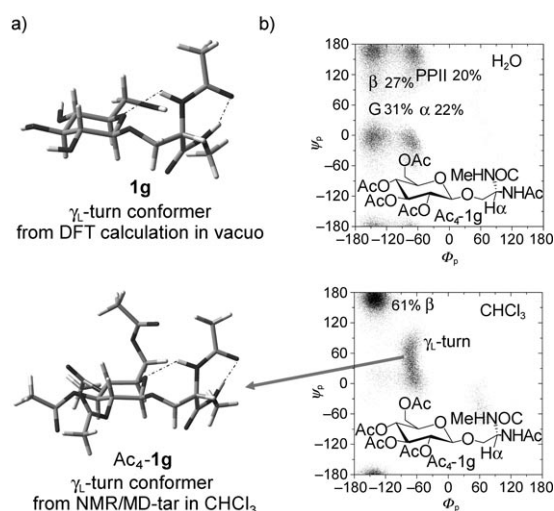


Figure 7. a) B3LYP/6-31+G(d) geometry of the minimum-energy conformation of **1g**. b) Φ_p/Ψ_p distributions obtained from the MD-tar simulations for **Ac₄-1g** in water (right-up) and chloroform (right-down), and the γ_L -turn conformer of **Ac₄-1g** obtained from the MD-tar simulation in chloroform (left-down).

Moreover, to corroborate the influence of water on the conformational preferences of the glycopeptides, we also synthesised the peracetylated derivative of **1g**, compound **Ac₄-1g** (see Supporting Information). Interestingly, this compound is totally soluble not only in chloroform but also in water, which makes it an attractive candidate for our purpose. The conformational study of this compound in both solvents, employing the NMR/MD protocol described above, revealed that compound **Ac₄-1g** exhibits similar conformational behaviour to **1g** in water (see Figures 3b and 7b). This fact has been previously described in the literature^[30] for different glycopeptides. Thus, regarding structure stabilization, the hydroxyl groups of the sugar moiety in **1g** can only act as hydrogen bonding acceptors, which is consistent with the existence of water-bridging molecules. On the other hand, as deduced from the NMR/MD data (Figure 7b), the conformational preferences of compound **Ac₄-1g** in chloroform considerably differs from those found in aqueous solution. In fact, in chloroform an important population of β -sheet coexists with a moderate population of γ_L -turn, which is predicted by DFT calculations in vacuo for **1g**. The γ_L -turn conformer is mainly stabilised by intramolecular hydrogen bonding.

Conclusion

β -D-O-Glycosylation produces a remarkable effect on the conformational behaviour of the peptide backbone of the model peptides investigated in this work. Indeed, it seems responsible for the observed shift from extended conformations (model peptides) towards the folded conformations (model glycopeptides). This conclusion has been solidly assessed by a combined NMR/MD protocol. Interestingly, the

MD results for the glycopeptides, together with those obtained for a peracetylated derivative, point towards the existence of water-bridging molecules between the sugar and peptide moieties that could explain the stabilization of α -helix and G conformers in aqueous solution. Furthermore, application of these approaches to larger systems will be considered in future work.

Experimental Section

General procedures: Solvents were purified according to standard procedures. Analytical TLC was performed by using Polychrom SI F254 plates. Column chromatography was performed by using silica gel 60 (230–400 mesh). ^1H and ^{13}C NMR spectra were recorded on a Bruker ARX 300 and Bruker Avance 400 spectrometer. ^1H and ^{13}C NMR spectra were recorded in CDCl_3 and D_2O with TMS as the external standard by using a coaxial microtube (chemical shifts are reported in ppm on the δ scale, coupling constants in Hz). Melting points were determined on a Büchi B-545 melting point apparatus and are uncorrected. Optical rotations were measured on a Perkin-Elmer 341 polarimeter. Microanalyses were carried out on a CE Instruments EA-1110 analyser and are in good agreement with the calculated values.

Ac-L-Ser(β -D-Glc)-NHMe (1g): Silver triflate (975 mg, 3.60 mmol) was added to a suspension of Ac-L-Ser-NHMe (**1**, 350 mg, 2.18 mmol) and powdered molecular sieves (4 Å, 1 g) in dichloromethane (5 mL) under an inert atmosphere. The mixture was stirred at -30°C and then 2,3,4,6-tetra-*O*-benzoyl- α -D-glucopyranosyl bromide (2 g, 3.03 mmol) in dichloromethane (2 mL) was added. The mixture was stirred at -30°C for 1 h and then was warmed at 25°C and stirred for 14 h. The crude was filtered, concentrated and purified by silica gel column chromatography, with dichloromethane/methanol 95:5 as the eluent to yield 821 mg (51%) of Ac-L-Ser(β -D-Bz₄Glc)-NHMe as a white solid. A solution of this compound (355 mg, 0.48 mmol) in methanol (10 mL) was treated with a 0.5 M solution of sodium methoxide in methanol (0.1 mL). After stirring for 3 h, the mixture was neutralised with Dowex 50-X8, filtered and concentrated. Purification of the residue with C₁₈ reverse-phase sep-pak cartridge gave 141 mg (91%) of **1g**. $[\alpha]_{\text{D}}^{25} = +2.7$ ($c=0.53$, CH_3OH); ^1H NMR (400 MHz, D_2O) $\delta=2.04$ (s, 3H), 2.71 (s, 3H), 3.25 (dd, 1H, $J=8.1$ Hz, $J=9.2$ Hz), 3.31–3.36 (m, 1H), 3.39–3.48 (m, 2H), 3.68 (dd, 1H, $J=5.9$ Hz, $J=12.3$ Hz), 3.81–3.90 (m, 2H), 4.19 (dd, 1H, $J=5.2$ Hz, $J=10.6$ Hz), 4.42 (d, 1H, $J=7.9$ Hz), 4.48 ppm (t, 1H, $J=4.6$ Hz); ^{13}C NMR (100 MHz, D_2O): $\delta=21.8$, 26.0, 53.9, 60.7, 68.7, 69.5, 73.0, 75.6, 75.9, 102.2, 171.8, 174.5 ppm; elemental analysis calcd for C₁₂H₂₂N₂O₈: C 44.72, H 6.88, N 8.69; found: C 44.64, H 6.76, N 8.56.

Ac-L-Thr(β -D-Glc)-NHMe (2g): In a similar way to that described for **1g**, compound **2g** (101 mg, 27%) was obtained from **2** (120 mg, 0.68 mmol). $[\alpha]_{\text{D}}^{25} = -2.8$ ($c=1.35$, CH_3OH); ^1H NMR (400 MHz, D_2O): $\delta=1.23$ (d, 3H, $J=6.3$ Hz), 2.10 (s, 3H), 2.74 (s, 3H), 3.23 (dd, 1H, $J=8.2$, $J=9.2$ Hz), 3.34–3.50 (m, 3H), 3.71 (dd, 1H, $J=5.4$, $J=12.3$ Hz), 3.88 (dd, 1H, $J=1.6$, $J=12.3$ Hz), 4.35 (d, 1H, $J=3.4$ Hz), 4.39–4.46 (m, 1H), 4.50 ppm (d, 1H, $J=7.9$ Hz); ^{13}C NMR (100 MHz, D_2O): $\delta=15.7$, 21.7, 25.9, 58.4, 60.6, 69.5, 72.9, 73.3, 75.6, 75.7, 99.6, 172.2, 174.9 ppm; elemental analysis calcd for C₁₃H₂₄N₂O₈: C 46.42, H 7.19, N 8.33; found: C 46.37, H 7.10, N 8.42.

2D NMR experiments: NMR spectroscopic experiments were recorded on a Bruker Avance 400 spectrometer at 298 K. Magnitude-mode ge-2D COSY spectra were recorded with gradients and by using the cosygpf pulse program with 90° pulse width. Phase-sensitive ge-2D HSQC spectra were recorded by using z filter and selection before t1 removing the decoupling during acquisition by use of the invgpnrdp pulse program with CNST2 $J(\text{H,C})=145$ Hz. 2D NOESY experiments were made by using phase-sensitive ge-2D NOESY for CDCl_3 spectra and phase-sensitive ge-2D NOESY with WATERGATE for $\text{H}_2\text{O}/\text{D}_2\text{O}$ 9:1 spectra. Selective ge-1D NOESY experiments were carried out by using the 1D-DPFGE NOE pulse sequence.

Calculations

MD-tar simulations (dielectric constant=80): NOE-derived distances (see Tables 1 and 2) were included as time-averaged distance constraints, and scalar coupling constants J as time-averaged coupling constraints. A $\langle r^{-6} \rangle^{-1/6}$ average was used for the distances and a linear average was used for the coupling constants. Final trajectories were run by using an exponential decay constant of 8000 ps and a simulation length of 80 ns.

Molecular modelling in explicit water: The solute molecule was immersed in a bath TIP3P water molecules^[31] with the LEAP module.^[32] The simulation was performed by using periodic boundary conditions and the particle-mesh Ewald approach^[33] to introduce long-range electrostatic effects. The SHAKE algorithm^[34] for hydrogen atoms was employed and a 9 Å cutoff was applied to Lennard-Jones interactions. The 10 ns unrestrained MD trajectories were collected at constant pressure (1 atm) and temperature (300 K) and analysed by using the CARNAL module.^[35]

DFT calculations: The calculations were carried out by means of the B3LYP hybrid functional.^[26] Full optimizations, by using the 6-31+G(d) basis set, were carried out with the Gaussian 03 package.^[36] Analytical frequencies were calculated at the B3LYP/6-31+G(d) level to determine the nature of the optimised geometries.

Acknowledgements

This work was supported by the Ministerio de Educación y Ciencia and FEDER (project CTQ2005-06235/BQU and Ramón y Cajal contracts of F.C. and J.H.B.), the Universidad de La Rioja (project API-05/B01) and the Gobierno de La Rioja (ANGI-2004/03 and ANGI-2005/01 projects). The authors thank CESGA for computer support. F.C. and J.H.B. have contributed equally to this work.

- [1] a) P. Van den Steen, P. M. Rudd, R. A. Dwek, G. Opdenakker, *Crit. Rev. Biochem. Mol. Biol.* **1998**, *33*, 151–208; b) R. A. Dwek, *Chem. Rev.* **1996**, *96*, 683–720; c) C. M. Taylor, *Tetrahedron* **1998**, *54*, 11317–11362; d) H. Helzner, T. Reipen, M. Schultz, H. Kunz, *Chem. Rev.* **2000**, *100*, 4495–4537; e) K. C. Nicolaou, H. J. Mitchell, *Angew. Chem.* **2001**, *113*, 1624–1672; *Angew. Chem. Int. Ed.* **2001**, *40*, 1576–1624; f) M. R. Pratt, C. R. Bertozzi, *Chem. Soc. Rev.* **2005**, *34*, 58–68.
- [2] G. J. Strous, J. Dekker, *Crit. Rev. Biochem. Mol. Biol.* **1992**, *27*, 57–92.
- [3] a) G. W. Hart, R. S. Haltiwanger, G. D. Holt, W. G. Kelly, *Annu. Rev. Biochem.* **1989**, *58*, 841–874; b) B. K. Hayes, K. D. Greis, G. W. Hart, *Anal. Biochem.* **1995**, *228*, 115–122; c) R. S. Haltiwanger, W. G. Kelly, E. P. Roquemore, M. A. Blomberg, L.-Y. D. Dong, L. Kreppel, T.-Y. Chou, K. Greis, G. W. Hart, *Biochem. Soc. Trans.* **1992**, *20*, 264–269.
- [4] a) H. Nishimura, S.-I. Kawabata, W. Kisiel, S. Hase, T. Ikenaka, T. Takao, Y. Shimonishi, S. Iwanaga, *J. Biol. Chem.* **1989**, *264*, 20320–20325; b) C. T. Kriss, B.-S. Lou, L. Z. Szabò, S. A. Mitchell, V. J. Hruby, R. Polt, *Tetrahedron: Asymmetry* **2000**, *11*, 9–25; c) C. M. Jackson, Y. Nemerson, *Annu. Rev. Biochem.* **1980**, *49*, 765–811; d) K. G. Mann, R. J. Jenny, S. Krishnaswamy, *Annu. Rev. Biochem.* **1988**, *57*, 915–956; e) S. Hase, H. Nishimura, S.-I. Kawabata, S. Iwanaga, T. Ikenaka, *J. Biol. Chem.* **1990**, *265*, 1858–1861; f) K. B. Reimer, M. Meldal, S. Kusumoto, K. Fukase, K. Bock, *J. Chem. Soc. Perkin Trans. 1* **1993**, 925–932; g) L. Shao, Y. Luo, D. J. Moloney, R. S. Haltiwanger, *Glycobiology* **2002**, *12*, 763–770.
- [5] a) S. A. Mitchell, M. R. Pratt, V. J. Hruby, R. Polt, *J. Org. Chem.* **2001**, *66*, 2327–2342; b) E. J. Bilsky, R. D. Egleton, S. A. Mitchell, M. M. Palian, P. Davis, J. D. Huber, H. Jones, H. I. Yamamura, J. Janders, T. P. Davis, F. Porreca, V. J. Hruby, R. Polt, *J. Med. Chem.* **2000**, *43*, 2586–2590.
- [6] a) D. H. Live, R. A. Kumar, X. Beebe, S. J. Danishefsky, *Proc. Natl. Acad. Sci. USA* **1996**, *93*, 12759–12761; b) D. M. Coltart, A. K. Royyuru, L. J. Williams, P. W. Glunz, D. Sames, S. Kuduk, J. B.

- Schwarz, X.-T. Chen, S. J. Danishefsky and D. H. Live, *J. Am. Chem. Soc.* **2002**, *124*, 9833–9844.
- [7] a) M. M. Palian, N. E. Jacobsen, R. Polt, *J. Pept. Res.* **2001**, *58*, 180–189; b) M. M. Palian, V. I. Boguslavsky, D. F. O'Brien, R. Polt, *J. Am. Chem. Soc.* **2003**, *125*, 5823–5831.
- [8] O. Seitz, *ChemBioChem* **2000**, *1*, 214–246.
- [9] S. Gnanakaran, A. E. García, *J. Phys. Chem. B* **2003**, *107*, 12555–12557.
- [10] a) E. E. Simanek, D.-H. Huang, L. Pasternack, T. D. Machajewski, O. Seitz, D. S. Millar, H. J. Dyson, C.-H. Wong, *J. Am. Chem. Soc.* **1998**, *120*, 11567–11575; b) W.-G. Wu, L. Pasternack, D.-H. Huang, K. M. Koeller, C.-C. Lin, O. Seitz, C.-H. Wong, *J. Am. Chem. Soc.* **1999**, *121*, 2409–2417; c) S. E. O'Connor, B. Imperiali, *J. Am. Chem. Soc.* **1997**, *119*, 2295–2296; d) P.-H. Tseng, W.-T. Jiaang, M.-Y. Chang, S.-T. Chen, *Chem. Eur. J.* **2001**, *7*, 585–590; e) D. Bailey, D. V. Renouf, D. G. Large, C. D. Warren, E. F. Hounsell, *Carbohydr. Res.* **2000**, *324*, 242–254; f) P. Braun, G. M. Davies, M. R. Price, P. M. Williams, S. J. B. Tendler, H. Kunz, *Bioorg. Med. Chem.* **1998**, *6*, 1531–1545; g) H. Matter, L. Szilagyi, P. Forgo, Z. Marinic, B. Klaić, *J. Am. Chem. Soc.* **1997**, *119*, 2212–2223; h) C. J. Bosques, S. M. Tschampel, R. J. Woods, B. Imperiali, *J. Am. Chem. Soc.* **2004**, *126*, 8421–8425; i) K. Fehér, P. Pristovsek, L. Szilagyi, D. Ljevakovic, J. Tomasic, *Bioorg. Med. Chem.* **2003**, *11*, 3133–3140; j) H. Moller, N. Serttas, H. Paulsen, J. M. Burchell, J. Taylor-Papadimitriou, B. Meyer, *Eur. J. Biochem.* **2002**, *269*, 1444–1455; k) P. Bour, M. Budesinsky, V. Spirko, J. Kapitan, J. Sebestik, V. Sychrovsky, *J. Am. Chem. Soc.* **2005**, *127*, 17079–17089; l) A. Perczel, E. Kollát, M. Hollósi, G. D. Fasman, *Biopolymers* **1993**, *33*, 665–685; m) E. Lang, B. Hargittai, Z. Majer, A. Perczel, M. Mak, M. KajtarPeredy, L. Radics, G. D. Fasman, M. Hollosi, *Protein Pept. Lett.* **1996**, *3*, 9–16.
- [11] a) R. Liang, A. Andreotti, D. Kahne, *J. Am. Chem. Soc.* **1995**, *117*, 10395–10396; b) M. Gobbo, A. Nicotra, R. Rocchi, M. Crisma, C. Toniolo, *Tetrahedron* **2001**, *57*, 2433–2443; c) L. Biondi, F. Filira, M. Gobbo, E. Pavin, R. Rocchi, *J. Pept. Sci.* **1998**, *4*, 58–71; d) M. Cudic, H. C. J. Ertl, L. Otvos, Jr., *Bioorg. Med. Chem.* **2002**, *10*, 3859–3870; e) L. Stella, M. Venanzi, M. Carafa, E. Maccaroni, M. E. Straccamore, G. Zanotti, A. Palleschi, B. Pispisa, *Biopolymers* **2002**, *64*, 44–56.
- [12] D. A. Pearlman, *J. Biomol. NMR* **1994**, *4*, 1–16.
- [13] H. J. Dyson, P. E. Wright, *Annu. Rev. Biophys. Chem.* **1991**, *20*, 519–538.
- [14] T. Haselhorst, T. Weimar, T. Peters, *J. Am. Chem. Soc.* **2001**, *123*, 10705–10714.
- [15] a) A. Marco, M. Llinas and K. Wuthrich, *Biopolymers* **1978**, *17*, 617–636; b) G. W. Vuister, A. Bax, *J. Am. Chem. Soc.* **1993**, *115*, 7772–7777.
- [16] D. A. Pearlman, D. A. Case, J. W. Caldwell, W. R. Ross, T. E. Cheatham III, S. DeBolt, D. Ferguson, G. Seibel, P. Kollman, *Comput. Phys. Commun.* **1995**, *91*, 1–41.
- [17] W. D. Cornell, P. C. Cieplack, I. Bayly, I. R. Gould, K. Merz, D. M. Ferguson, D. C. Spellmeyer, T. Fox, J. W. Caldwell, P. A. Kollman, *J. Am. Chem. Soc.* **1995**, *117*, 5179–5197.
- [18] R. J. Woods, R. A. Dwek, C. J. Edge, B. Fraser-Reid, *J. Phys. Chem.* **1995**, *99*, 3832–3846.
- [19] J. M. Wang, P. Cieplak, P. A. Kollman, *J. Comput. Chem.* **2000**, *21*, 1049–1074. For a recent review in this field see: J. W. Ponder, D. A. Case, *Adv. Protein Chem.* **2003**, *66*, 27–85.
- [20] C. Simmerling, B. Strockbine, E. Roitberg, *J. Am. Chem. Soc.* **2002**, *124*, 11258–11259.
- [21] Y. Mu, D. S. Kosov, G. Stock, *J. Phys. Chem. B* **2003**, *107*, 5064–5073.
- [22] Letter code employed in S. S. Zimmerman, M. S. Pottle, G. Némethy, H. A. Scheraga, *Macromolecules* **1977**, *10*, 1–9; In this work the β conformer is referred to as E, the PPII as F and the α -helix conformation as A.
- [23] a) V. J. Hruby, G. Li, C. Haskell-Luevano, M. Shenderovich, *Biopolymers* **1997**, *43*, 219–266; b) V. J. Hruby, P. M. Balse, *Curr. Med. Chem.* **2000**, *7*, 945–970.
- [24] G. R. J. Thatcher, *The Anomeric Effect and Associated Stereoelectronic Effects*, American Chemical Society, Washington, DC, **1993**.
- [25] a) F. Corzana, M. S. Motawia, C. Hervé du Penhoat, S. Pérez, S. M. Tschampel, R. J. Woods, S. B. Engelsen, *J. Comput. Chem.* **2004**, *25*, 573–586; b) S. W. Rick, B. J. Berne, *J. Am. Chem. Soc.* **1996**, *118*, 672–679; c) J. Gao, M. Freindorf, *J. Phys. Chem. A* **1997**, *101*, 3182–3188; d) D. Beglov, B. Roux, *J. Phys. Chem. B* **1997**, *101*, 7821–7826; e) M. Buck, M. Karplus, *J. Phys. Chem. B* **2001**, *105*, 11000–11015; f) W. Rocha, K. D. Almeida, K. Coutinho, S. Canuto, *Chem. Phys. Lett.* **2001**, *345*, 171–178; g) S. Iuchi, A. Morita, S. Kato, *J. Phys. Chem. B* **2002**, *106*, 3466–3476; h) F. Corzana, M. S. Motawia, C. Hervé du Penhoat, F. van der Berg, A. Blennow, S. Pérez, S. B. Engelsen, *J. Am. Chem. Soc.* **2004**, *126*, 13144–13155.
- [26] C. A. Andersson, S. B. Engelsen, *J. Mol. Graphics Modell.* **1999**, *17*, 101–105.
- [27] M. J. S. Dewar, E. G. Zoebisch, E. F. Healy, J. J. P. Stewart, *J. Am. Chem. Soc.* **1985**, *107*, 3902–3909.
- [28] a) C. Lee, W. Yang, R. Parr, *Phys. Rev. B* **1988**, *37*, 785–789; b) A. D. Becke, *J. Chem. Phys.* **1993**, *98*, 5648–5652.
- [29] G. I. Csonka, G. A. Schubert, A. Perczel, C. P. Sosa, I. G. Csizmadia, *Chem. Eur. J.* **2002**, *8*, 4718–4732.
- [30] Y. Mimura, Y. Inoue, N. J. Maeji, R. Chūjō, *Int. J. Pept. Protein Res.* **1989**, *34*, 363–368.
- [31] M. Chianson, N. A. Baner, J. Simpson, J. A. McCammon, *J. Am. Chem. Soc.* **2002**, *124*, 1438–1442.
- [32] C. E. A. F. Schafmeister, W. F. Ross, V. Romanovsky, University of California, San Francisco, 1995.
- [33] C. S. A. T. Darden, *Annu. Rev. Biophys. Biomol. Struct.* **1999**, *28*, 155–179.
- [34] J. P. Ryckaert, G. Ciccote, J. C. Berendsen, *J. Comp. Physiol.* **1977**, *23*, 327–341.
- [35] W. S. Ross, Carnal: coordinate Analysis Program, University of California, San Francisco, Department of Pharmaceutical Chemistry.
- [36] Gaussian 03 (Revision B.05), M. J. Frisch, G. W. Trucks, H. B. Schlegel, G. E. Scuseria, M. A. Robb, J. R. Cheeseman, J. A. Montgomery, Jr., T. Vreven, K. N. Kudin, J. C. Burant, J. M. Millam, S. S. Iyengar, J. Tomasi, V. Barone, B. Mennucci, M. Cossi, G. Scalmani, N. Rega, G. A. Petersson, H. Nakatsuji, M. Hada, M. Ehara, K. Toyota, R. Fukuda, J. Hasegawa, M. Ishida, T. Nakajima, Y. Honda, O. Kitao, H. Nakai, M. Klene, X. Li, J. E. Knox, H. P. Hratchian, J. B. Cross, C. Adamo, J. Jaramillo, R. Gomperts, R. E. Stratmann, O. Yazyev, A. J. Austin, R. Cammi, C. Pomelli, J. W. Ochterski, P. Y. Ayala, K. Morokuma, G. A. Voth, P. Salvador, J. J. Dannenberg, V. G. Zakrzewski, S. Dapprich, A. D. Daniels, M. C. Strain, O. Farkas, D. K. Malick, A. D. Rabuck, K. Raghavachari, J. B. Foresman, J. V. Ortiz, Q. Cui, A. G. Baboul, S. Clifford, J. Cioslowski, B. B. Stefanov, G. Liu, A. Liashenko, P. Piskorz, I. Komaromi, R. L. Martin, D. J. Fox, T. Keith, M. A. Al-Laham, C. Y. Peng, A. Nanayakkara, M. Challacombe, P. M. W. Gill, B. Johnson, W. Chen, M. W. Wong, C. Gonzalez, and J. A. Pople, Gaussian, Inc., Pittsburgh PA, **2003**.

Received: January 30, 2006

Revised: May 11, 2006

Published online: July 19, 2006